UTM Faculty of Mechanical Engineering UNIVERSITI TEKNOLOGI MALAYSIA
THE ENGINEER STORY

e-ISSN: 3009 - 0792 Volume 16, 2025, 13-17

AERODYNAMICS STUDY ON BLUNT-EDGED DELTA WING VFE-2 CONFIGURATION AT LOW REYNOLDS NUMBER

Afif Izhar Abdullah Haris [*], Haris Ahmad Israr Ahmad, Shabudin Mat
Faculty of Mechanical Engineering, Universiti Teknologi Malaysia,
81310 UTM Johor Bahru, Johor, Malaysia.
[*] Corresponding author: afifizhar@graduate.utm.my

ABSTRACT

This study examines the aerodynamic behaviour of a blunt-edged delta wing based on the Vortex Flow Experiment 2 (VFE-2) configuration under low Reynolds number conditions. The investigation focuses on the effects of varying angle of attack (0° to 21°), yaw angle (−10° to +10°), and freestream velocity (25 m/s and 30 m/s) on aerodynamic forces, moments, and surface pressure distribution. Experiments were conducted in a low-speed wind tunnel, with solid blockage corrections applied using the Maskell method. The results show clear trends in lift, drag, and pitching moment coefficients, with the highest lift-to-drag ratio occurring at moderate angles of attack. Pressure measurements confirm the development of leading-edge vortices at higher angles, while yaw introduces asymmetry in vortex strength, influencing aerodynamic stability. These insights contribute to a deeper understanding of vortex-dominated flows at low Reynolds numbers and support the aerodynamic design of micro air vehicles (MAVs) and unmanned aerial systems (UAS).

KEYWORD

Blunt-edged delta wing, vortex flow, Reynolds number, aerodynamic forces

INTRODUCTION

The experiment was conducted in the Open-Loop Low-Speed Wind Tunnel (UTM OL-LST) at UTM Aerolab. The test section measures 457 mm × 457 mm × 1270 mm, with a maximum freestream velocity of 30 m/s, suitable for low Reynolds number studies. A JR3 six-axis load balance measured aerodynamic forces and moments, with the VFE-2-based delta wing model mounted on a single-strut support allowing angle of attack and yaw adjustments. The model featured a 65° leading-edge sweep and blunt apex, scaled down 1:4.075 to fit the tunnel while preserving geometric similarity. Its mean aerodynamic chord (MAC) was 0.2167 m. Seven pressure taps along the leading edge (Y/Cr = 10% to 80%) were connected to an FKPS 30P electronic pressure scanner. The model was 3D printed for precision and measurement compatibility. Tests were conducted at 30 m/s, yielding Re ≈ 0.42×10^6 ($\rho = 1.17$ kg/m³, $\mu = 1.81 \times 10^{-5}$ Pa·s). Freestream velocity was verified with a tube anemometer, and pressure systems calibrated using a digital manometer. Tare readings were taken before each run. Data were collected after flow stabilization, with angles of attack from 0° to 21° (3° steps) and yaw angles of –10°, 0°, and +10°, sampled at 10 Hz. Solid blockage corrections were applied using the Maskell method, enabling accurate analysis of surface pressure and vortex behaviour under combined pitch and yaw.

MATERIAL AND METHODOLOGY

The experiment was conducted in the Open-Loop Low-Speed Wind Tunnel (UTM OL-LST) at UTM Aerolab. The test section measured 457 mm × 457 mm × 1270 mm, with a maximum freestream velocity of 30 m/s, ideal for low Reynolds number studies. A JR3 six-axis load balance measured aerodynamic forces and moments, with the model mounted on a single-strut support allowing angle of attack and yaw adjustments. The delta wing model followed the VFE-2 configuration, with a 65° leading-edge sweep and blunt apex, scaled down by 1:4.075 to maintain geometric similarity. The mean aerodynamic chord (MAC) was 0.2167 m. Seven pressure taps were placed along the leading edge from Y/Cr = 10% to 80%, connected to an FKPS 30P electronic pressure scanner. The model was 3D printed for precision and system compatibility. Tests were performed at 30 m/s, giving a Reynolds number of ~0.42×10^6, based on air density of 1.17 kg/m^3 and dynamic viscosity of 1.81×10^{-5} Pa.s. Freestream velocity was verified with a tube anemometer, and pressure systems were calibrated using a digital manometer. Tare readings were taken before data collection to remove baseline offsets. Data were collected after flow stabilization at angles of attack from 0° to 21° in 3° steps, and yaw angles of –10°, 0°, and +10°, with measurements sampled at 10 Hz. Solid blockage corrections were applied using the Maskell method. This setup enabled detailed analysis of surface pressure and vortex behaviour under combined pitch and yaw conditions.

RESULT AND DISCUSSION

Figures 2 and 3 illustrate that the aerodynamic performance of a blunt-edged delta wing is significantly influenced by angle of attack (AoA), Reynolds number, and yaw angle. At a Reynolds number of $Re = 0.35 \times 10^6$, the lift coefficient increases with AoA up to approximately $\alpha = 12^o$, after which it decreases due to vortex breakdown. Drag rises sharply beyond $\alpha = 15^o$, and the pitching moment becomes increasingly negative at higher angles of attack, particularly under yaw angles of ±10°, suggesting reduced longitudinal and directional stability. The lift-to-drag ratio reaches its peak at $\alpha = 6^o$, but declines rapidly thereafter, indicating a swift loss in aerodynamic efficiency. Yaw introduces notable asymmetries in the flow field. At ±10° yaw, lift decreases due to weakened leeward vortices, while drag increases as a result of uneven vortex shedding. The pitching moment also shifts, reflecting greater instability under yawed conditions.

At a higher Reynolds number of $Re = 0.42 \times 10^6$, similar trends are observed but occur at higher angles of attack. Lift continues to rise until approximately $\alpha = 18^o$drag increases more gradually, and the lift-to-drag ratio peaks around $\alpha = 7^o$ before declining more smoothly. Yaw effects remain present but are less pronounced, indicating enhanced vortex stability and reduced sensitivity to crossflow disturbances at the higher Reynolds number.

The dotted circles shown in Figure 4 are used as visual indicators to emphasize significant aerodynamic events occurring along the pressure coefficient (C_p) curves. These events include phenomena such as vortex breakdown, flow separation, and boundary layer reattachment. By highlighting these specific points, the markers assist in identifying key shifts in pressure distribution that signal important changes in the underlying flow behaviour. At the leading-edge spanwise station (Y/Cr = 0.1), the dotted circle typically marks the point where the suction peak starts to flatten or reverse, generally observed between angles of attack $\alpha = 15^o$ and 18^o. This change indicates the beginning of vortex breakdown, a stage at which the primary vortex begins to lose stability due to increasing adverse pressure gradients.

At this location, the suction peak intensifies with rising angle of attack, suggesting robust vortex formation near the wing's apex. The influence of Reynolds number is also noticeable where higher values, such as $Re = 0.42 \times 10^6$, lead to stronger suction effects and a delayed vortex breakdown compared to lower values like $Re = 0.35 \times 10^6$At the mid-span position (Y/Cr = 0.4), the dotted circle highlights a later emergence of the suction peak, usually occurring between $\alpha = 18^o$ and 21^o. Here, the increase in suction is more gradual than at the leading edge, affected by the formation of secondary vortices and variations in spanwise pressure gradients. The trend suggests that higher Reynolds numbers continue to postpone flow reversal while enhancing suction strength. At the trailing-edge region (Y/Cr = 0.8), the dotted circle identifies an earlier flattening of the suction peak, with reversal typically happening between $\alpha = 12^o$ and 15^o. This suggests that flow separation dominates in this area. Beyond this angle, pressure recovery becomes more prominent as boundary layer detachment increases, signalling a shift into fully separated flow.

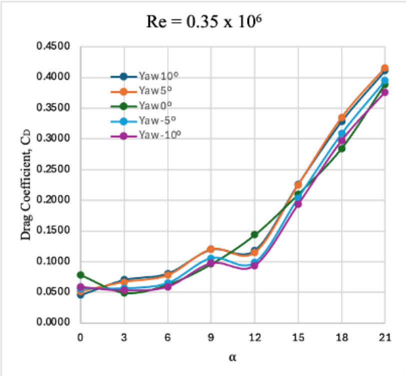

(a) Drag Coefficient

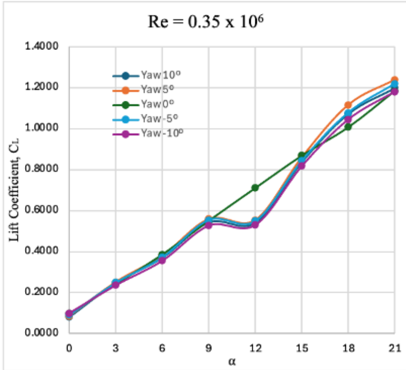

(b) Lift Coefficient

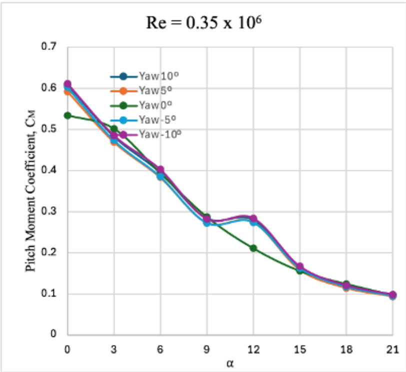

(c) Pitching Moment Coefficient

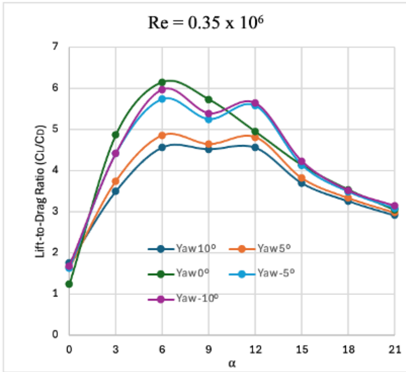

(d) Lift-to-Drag Ratio Coefficient

Figure 1: Effect of aerodynamic coefficient at R = 0.35×10^6

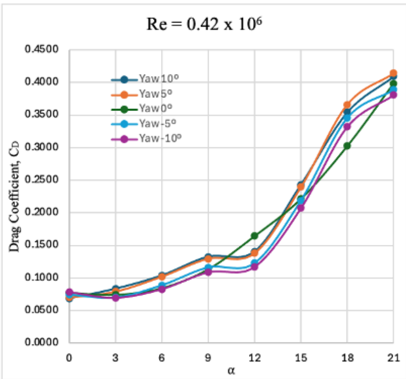

(a) Drag Coefficient

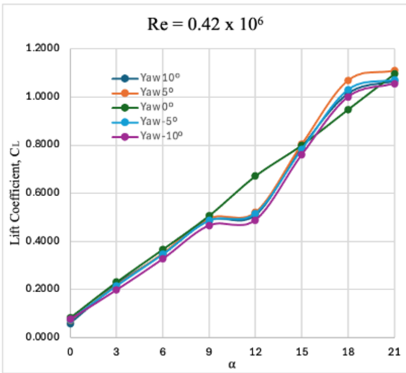

(b) Lift Coefficient

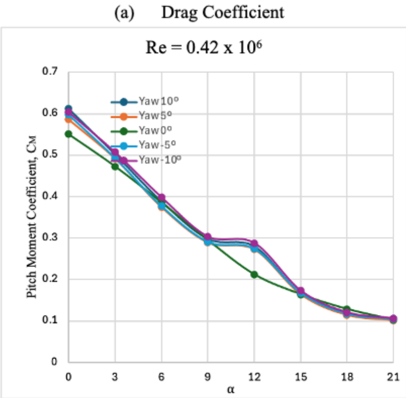

(c) Pitching Moment Coefficient

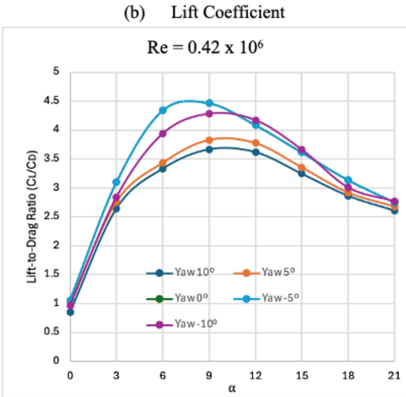

(d) Lift-to-Drag Ratio Coefficient

Figure 2 Effect of aerodynamic coefficient at R = 0.42×10^6

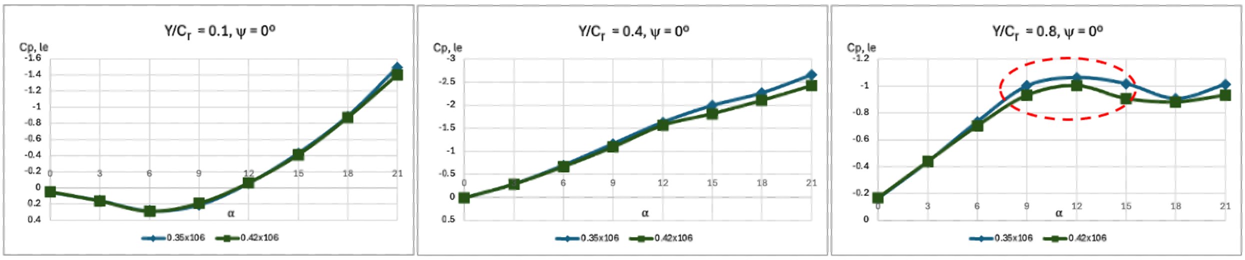

Figure 3: Pressure distribution at $\psi = 0^{o}$

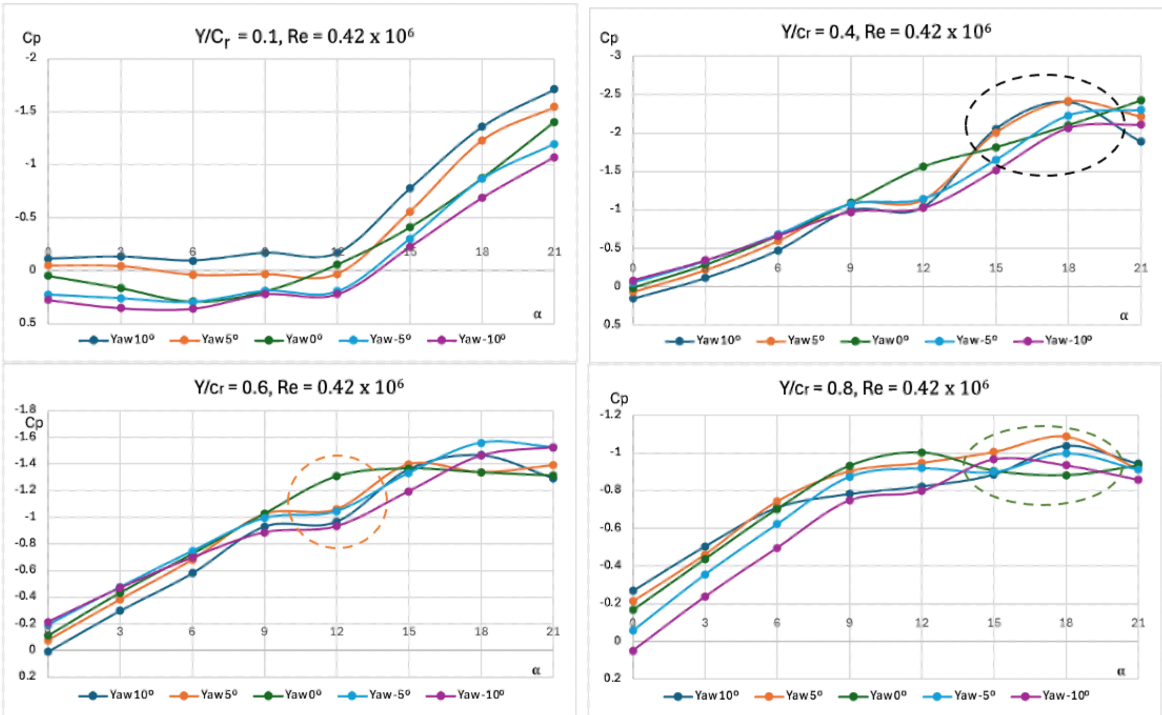

Figure 4: Pressure distribution along leading edge at various α and ψ angle with Re = 0.42×10^6

Figure 5 illustrates how pressure changes along the leading edge of the VFE-2 delta wing at Re = 0.42×10^6, focusing on how yaw angle (ψ) affects flow at different spanwise points (Y/Cr = 0.1, 0.4, 0.6, and 0.8). The results highlight how pitch (α) and yaw work together to shape vortex strength, suction peaks, and flow separation along the wing. Near the leading edge (Y/Cr = 0.1), suction increases steadily with α, especially when the wing faces into the yaw (ψ = +5° and +10°). This suggests stronger vortex formation on the windward side. However, beyond α = 15° to 18°, the suction levels off, indicating the start of vortex breakdown. Further back at Y/Cr = 0.4, suction grows more slowly, but yaw still plays a big role. Positive yaw speeds up vortex formation, while negative yaw delays it. A sharp rise in Cp around α = 18° marks the onset of flow detachment. At Y/Cr = 0.6, the vortex influence starts to fade. Still, secondary vortices briefly reattach the boundary layer before final separation, helping to maintain some suction, especially on the windward side. By the time the flow reaches the trailing edge (Y/Cr = 0.8), the effects of yaw mostly disappear. The pressure curves start to overlap, showing that the vortices have broken down and separation dominates, typically around α = 12° to 15°. To make these changes clearer, Figure 6 includes dotted circles: black for vortex breakdown at Y/Cr = 0.4, orange for brief reattachment at Y/Cr = 0.6, and green for full separation at Y/Cr = 0.8.

CONCLUSION

In summary, this study successfully analysed the aerodynamic performance of the VFE-2 blunt-edged delta wing at low Reynolds numbers. The results underscore the strong impact of angle of attack, yaw angle, and Reynolds number on vortex behaviour, flow separation, and aerodynamic force generation. Pressure distribution patterns revealed key flow phenomena, including vortex breakdown, boundary layer reattachment, and full separation. These insights deepen our understanding of vortex-driven aerodynamics and contribute to the design of more efficient micro air vehicles and unmanned aerial systems. Future work on flow control strategies may further enhance performance in practical flight conditions.

ACKNOWLEDGEMENT

The authors gratefully acknowledge the support of the UTM Aerolab technical staff, particularly Encik Salahuddin, for his invaluable assistance in the setup and execution of the wind tunnel experiments. Special thanks are also extended to Assoc. Prof. Ir. Dr. Shabudin Mat for their guidance and significant contributions to the data collection and analysis process.

REFERENCE

Dwivedi, Y. D., Navaneetha, C., & Bhargava, V. (2022). Flow analysis on delta wing – A review. Graduate Research in Engineering and Technology, 1–8. https://doi.org/10.47893/gret.2022.1071

Luckring, J. M., & Hummel, D. (2013). What was learned from the new VFE-2 experiments. Aerospace Science and Technology, 24(1), 77–88. https://doi.org/10.1016/j.ast.2011.07.012

Madan, I., Tajuddin, N., Said, M., Mat, S., Othman, N., Wahid, M. A., Radzi, N. H. M., Miau, J. J., Chen, Y. R., & Chen, L. Y. (2021). Influence of Active Flow Control on Blunt-Edged VFE-2 Delta Wing model. International Journal of Automotive and Mechanical Engineering, 18(1), 8411–8422. https://doi.org/10.15282/ijame.18.1.2021.01.0636

Said, M., Imai, M., Mat, S., Nasir, N., Kasim, K. A., Nik Mohd, N. A. R., & Mansor, S. (2020). Tuft Flow Visualisation on UTM-LST VFE-2 Delta Wing Model Configuration at High Angle of Attacks. International Journal of Automotive and Mechanical Engineering, 17(3), 8214–8223. https://doi.org/10.15282/IJAME.17.3.2020.15.0619

Tajuddin, N., Mat, S., & Said, M. (2020). Tomography Systems and Sensor Applications Flow Visualization Above Blunt-Edged Delta Wing. In Journal of Tomography System & Sensors Application (Vol. 3).